



Historical trend analysis and future projections of precipitation from CMIP5 models in the Alborz mountain area, Iran

Mohammad Zarenistanak¹

Received: 12 January 2017 / Accepted: 23 August 2018 / Published online: 1 September 2018
© Springer-Verlag GmbH Austria, part of Springer Nature 2018

Abstract

Precipitation changes in annual and seasonal time series over the Alborz Mountains area during 1950–2014 were analyzed using historical observations from 154 rain gauge stations. The projected changes in precipitation for the twenty-first century were evaluated using three Coupled Model Intercomparison Project Phase 5 (CMIP5) datasets. Trends in the precipitation time series were detected by linear regression and its significance was tested by *t* test. Mann–Kendall rank test (MK test) and Sen's slope estimator were also employed to confirm the results. Sequential Mann–Kendall test (SQ-MK test) was also applied for change point detection in annual and seasonal precipitation time series. Pre-whitening was used to eliminate the influence of serial correlation on the MK test. Future precipitation was analyzed by GFDL-CM3, HadGEM2-AO and MPI-ESM-MR models under two representative concentration pathways (RCP) RCP 4.5 and RCP 8.5 scenarios. The analysis of the historical precipitation series indicated an insignificant trend in the annual and seasonal series at most stations. The highest numbers of stations with negative significant trends occurred in winter and with positive significant trends in summer. The results of change point detection in annual and seasonal precipitation series show that most of the significant mutation points began in the 1970s. The future projections showed that precipitation may decrease according to most of the models under the RCP 4.5 and RCP 8.5 scenarios, while the decrease may not be large, except in the summer season for the end of this century.

1 Introduction

Trend analysis and projections of precipitation, on both the regional and global scales, have attracted attention among climatologists and governments who would come up with more accurate plans using the results. Such plans, particularly in arid and semi-arid regions such as Iran, could benefit hugely from these results.

Iranian economic and industrial progress has taken a faster pace in the last five decades. Fuels such as oil, natural gas and coal have been used in greater amounts. Accordingly, emission of CO₂ and other greenhouse gases has been on the rise. Such trends can lead to an increase in temperature and changes in precipitation patterns and the hydrologic cycle. In addition, population growth since the 1970s has put further pressure on land use, agricultural enterprises, livestock farming and solid/liquid waste generation, all of

which are responsible for environmental concerns such as climate change (Amiri and Eslamian 2010).

In Iran, the Alborz Mountains area receive the highest amount of precipitation for which several dams have been constructed to store water for agriculture and drinking purposes during summers. Local industries are dependent on farming and husbandry with 65% of the population engaged in related professions. It implies that agriculture and husbandry are directly affected by changes in precipitation pattern. In addition, the area of Hyrcanian forests covering the Alborz Mountain ranges is subject to decline in response to the changes in precipitation patterns. Previous studies show an increasing temperature trend in Asia which will continue in the twenty-first century. However, specifying a uniform precipitation pattern for Asia is not straightforward, because of unreliable and short data as well as different outputs of projection models (IPCC 2014). This shows the importance of precipitation analysis for this region for better management of water resources. Recent droughts have negatively affected Iran's economy. Therefore, studying the precipitation changes in the past decades and developing a prediction model for the twenty-first century is highly rewarding research topics for Iranian climatologists.

Responsible Editor: J.-T. Fasullo.

✉ Mohammad Zarenistanak
zareclima@gmail.com

¹ Research Institute of Shakhes Pajouh, Isfahan, Iran

Trend analysis and projections of precipitation series on the global as well as the regional scales have been investigated by many researchers throughout the world. Reviews can be found in Liu et al. (2012), Ramos et al. (2012), Ay and Kisi (2015), Sharmila et al. (2015), Palomino-Lemus et al. (2015), Jiang et al. (2015), Zhao et al. (2015), Eccel and Tomozeiu (2015), Palizdan et al. (2016) and Hu et al. (2016). Chen et al. (2011) highlighted a general increasing trend in annual precipitation in the arid region of Central Asia from 1930 to 2009. Terink et al. (2013) found that annual precipitation will decrease for the majority of the Middle East and Northern Africa region for the periods 2020–2030 and 2040–2050, with the decreases of 15–20% for the latter period. Deng et al. (2013) used nine CMIP5 datasets under different RCPs scenarios for the projections of spring and summer precipitation for the period 2013–2050 over the Yangtze River basin, China. The precipitation projections show significant positive linear trends of spring precipitation under the RCP2.6 and RCP8.5 scenarios, whereas summer precipitation will mainly undergo an inter-annual change. Yao and Chen (2015) reported a significant rising trend at a rate of 4.44 mm/decade and step change points in 1991 in annual precipitation for the Syr Darya basin during 1881–2011. Meshram et al. (2016) used MK test, Spearman's rho and Sen's slope estimator to identify precipitation trends in Chhattisgarh State, India. Results showed a significant decreasing trend at the 5% significance level in annual precipitation at most of the stations according to these tests. Chandniha et al. (2016) applied MK test, Sen's slope estimator and Mann–Whitney tests for trend detection in annual precipitation at 18 meteorological stations in Jharkhand State, India. The result showed a decreasing trend in annual precipitation at 5 out of 18 stations during the whole period.

Iran, with an area of 1,648,000 km², is located in the southwest of the Middle East which is situated in the mid-latitude belt of arid and semi-arid regions. The climate of Iran is arid or semi-arid except the coastal areas of the Caspian Sea and the foothill of the Alborz and Zagros Mountains. The average amount of precipitation over the country is 252 mm/year, which is less than one-third of the world average (Alizadeh and Keshavarz 2005). Precipitation in Iran has a high spatial and time variability. There are regions in the south of the Caspian Sea and some parts of the Zagros Mountains area which receive annual precipitation between 1200 and 2000 mm, whereas portions of the central part of Iran and Dasht-e Loot get less than 50 mm (Shifteh Some'e et al. 2012). Most of the precipitation falls during the winter and autumn seasons, due to the prevalence of humid westerly winds of the Mediterranean Sea.

Delju et al. (2013) applied statistical techniques to detect trends in precipitation series. The results indicated that mean precipitation increased at the rate of 9.2% from 1966 to 2005 over the Urmia Lake basin in the northwest of Iran.

Zarenistanak et al. (2014a) reported insignificant trends in annual and seasonal precipitation series at most of the stations located in the southwest of Iran. Arbabi Sabzevari et al. (2015) concluded no long-term trends in annual and monthly precipitation series in the southwestern Iran. Feizi et al. (2014) applied MK test for trend detection in precipitation series over Iran from 1969 to 2008. The results indicated that precipitation during summer and autumn had a negative trend in the southeastern parts of Iran which was stronger than the trend in spring, but no significant trend was detected in winter. Farhangi et al. (2016) revealed a decreasing trend in mean annual precipitation series at six out of ten stations located in western Iran. The temporal changes in precipitation and other climatic variables in Iran have also been found in several studies (e.g., Rahimzadeh et al. 2009; Sheikha and Bahremanda 2011; Dinpashoh et al. 2011; Tabari et al. 2011; Kousari et al. 2011; Tabari et al. 2012a; Tabari and Aghajanloo 2013; Tabari et al. 2014; Abghari et al. 2013; Zarenistanak et al. 2015).

Climate models could be useful tools to project climate variables. The World Climate Research Program Coupled Model Intercomparison Project not only provides a foundation for research groups to develop their Earth system models, but also contains more than 20 model datasets. CMIP has motivated using numerous researchers to project global and regional climate changes (Deng et al. 2013). The projection of precipitation changes in the Alborz Mountains has not received considerable attention from the government. In this paper, precipitation projections in the Alborz Mountains area during the twenty-first century by three models under the RCP4.5 and RCP8.5 scenarios are analyzed. A number of papers have reported regional climate change simulations over some part or the whole extent of Iran. Jafari (2012) highlighted a future winter precipitation increase of 10% and a summer precipitation decrease of 20% in the west of Gilan Province in the north of Iran under the A1B scenario from 2090 to 2099. Roshan and Grab (2012) used MAGICC/SCENGEN 5.3 compound model for precipitation projection over Iran. The results revealed that by the year 2100, the mean precipitation may increase by 36% relative to the period 1961–1990. Dhorde et al. (2014) found insignificant trends in annual and seasonal precipitation series over the southwest of Iran. The highest numbers of stations with significant trends occurred in winter. Results for the future projections showed that precipitation may decrease according to the majority of the models under the B1 and A1B scenarios, but the magnitude of this decrease may not be large, except for the MIROC model by 2100. Babaeiana et al. (2015) used PRECIS regional climate model for precipitation projection over Iran. Results showed a decrease in mean annual precipitation toward the end of the twenty-first century by 7.8 mm in the B2 scenario and 10.1 mm in the A2 scenario, with a maximum regional decrease of 100 mm in

the southeast of the Caspian Sea. Nazemosadat et al. (2016) reported that under the 20C3M scenario, precipitation may decrease by about 20% in the southern part of Iran in comparison to the historical time series.

Previous studies carried out in Iran only focused on precipitation trend analysis or projections. In this study, several statistical tests were used for trend detection in precipitation series and also three models under two scenarios were applied for precipitation projections to find out how global warming impacts the precipitation of the study area. This study focused on two main objectives. The first one was to detect the trends in the annual and seasonal precipitation over the Alborz Mountains area using the linear regression, the MK test, the SQ-MK test and the Sen’s slope estimator for the period 1950–2014. The second one is to project precipitation using GFDL-CM3, HadGEM2-AO and MPI-ESM-MR models under the RCP4.5 and RCP8.5 emissions scenarios over the study area.

2 Methodology

2.1 Study area and data

The Alborz Mountains area covers the northern part of Iran, particularly the provinces of East Azerbaijan, Ardebil, Zanjan, Qazvin, Tehran, Gilan, Mazandaran, Semnan and Golestan. The study area is located between 35°52’N and 39°26’N latitude, and 45°7’E and 56°3’E longitude. Having an approximate area of 207,221 km², it covers about 14% of the country land area (Fig. 1). The elevation ranges from –20 m in the coastal areas of the Caspian Sea to over 5671 m in Damavand Mountain. Damavand Mountain as the highest mountain in Iran is located in the central Alborz Mountain range. These mountains avoid the Caspian Sea moisture-bearing systems by crossing through the central region of Iran. In these mountains,

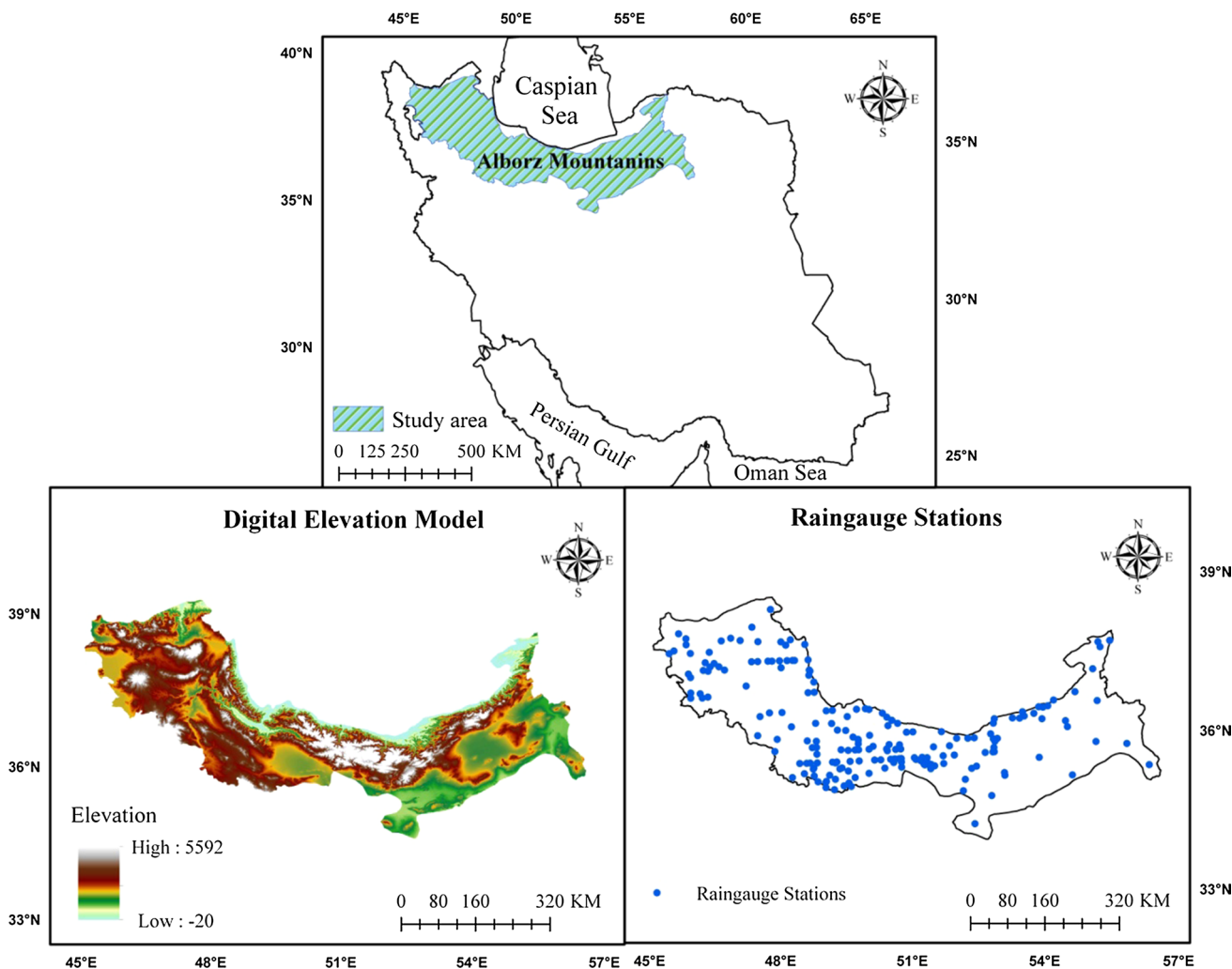


Fig. 1 Geographic location of the study area and spatial distribution of the rain gauge stations

several rivers originate. The rivers are generally fed by the snow accumulated in the mountains and the rainfall in the wet season. Generally, these rivers in this area can be divided into two categories. The rivers in the north foothill, such as Chalus River, Do Hezar River, Sardab River, Kojur River, Haraz River, Atrek River and Aras River, empty into the Caspian Sea. The second category is the rivers in the south Alborz Mountain foothill, of which the Alamut River, Shahrud River, Jajrood River and Lar River are the most important ones. The rivers from the latter category flow to the central part of Iran.

The north foothill of the Alborz Mountains is covered with the Hyrcanian forests. The forests cover about 55 km² of the southern shores of the Caspian Sea and Azerbaijan region. The economy of the region depends on fishing, industrial activities, agriculture, horticulture and animal husbandry. The region is a large producer of rice, grain and fruits. Most of the irrigation waters in the region are provided by precipitation.

For the period between 1950 and 2014, the precipitation data of 154 stations provided by the Islamic Republic of Iran Meteorological Organization (IRIMO) and Iranian Water Resources Management Organization were used for statistical analysis. The details of data availability for these 154 stations are reported in Table 1. The precipitation data were carefully checked for homogeneity and missing values. Missing values were estimated based on correlation analysis between the investigation station and the nearest station in its neighborhood. Homogeneity of the data was evaluated by the Pettitt's (Pettitt 1979) and Buishand range (Buishand 1982), the standard normal homogeneity (Alexandersson 1986) and the standard normal homogeneity by Alexandersson and Moberg (Alexandersson and Moberg 1997) tests. Thus, the homogeneity of the annual and seasonal precipitation series analyzed in this study has not been affected.

2.2 Precipitation characteristics

The Alborz Mountains area receives the highest amount of precipitation in Iran. The seasonal distribution of precipitation in this area is as follows: during autumn, the southwestern coasts of the Caspian Sea receive heavy precipitation thanks to winds coming from Siberia that create advective processes. In spring, the heights in the Azerbaijan region receive more precipitation due to foothill convections. During winter, there is relatively good precipitation in the whole area, thanks to western winds and humidity of the Mediterranean and Caspian seas. Winter precipitation is mainly snow, lasting some 3–5 months in the mountainous areas and 2–3 months on the coast of the Caspian Sea. The decreasing pattern of precipitation toward the Alborz heights shows that annual perspiration decreases from the coasts to the northern Alborz heights, although on the southern side it decreases

toward the lower lands. The eastern coasts of the Caspian Sea receive humid flows carried by western currents coming from the Gorgan valley into the east. Accordingly, the precipitation gradually decreases toward the east. This trend is accelerated to the point of sudden in toward the south and west, thanks to the Alborz Mountains. In the southwestern coasts, the maximum spots lie in seashores and inland in western coasts. This happens due to the presence of the impact of Siberian currents and sunlight. Precipitation variability over the Caspian Sea coasts is significantly influenced by the EL Niño-Southern Oscillation (ENSO) phases, the sea surface temperature (SST) and the intensity of the Siberian high (Nazemosadat and Ghasemi 2004; Nazemosadat 2001). The windward slopes of the Azerbaijan mountains receive more precipitation than the lower altitudes and the lee slopes (Alijani 1995).

2.3 Statistical tests for trend analysis

The statistical techniques used in the research are linear regression, MK test, SQ-MK test and Sen's slope estimator. The significance testing for all tests was performed at a 95% confidence level. These tests have been applied by many researchers for detection of the statistical significance of the trends in the climatological time series (e.g., Schlunzen et al. 2010; Tabari and Hosseinzadeh Talaei 2011b; Yavuz and Erdoğan 2012; Tabari et al. 2012b, 2016; Martinez et al. 2012; Hanif et al. 2013; Scardilli et al. 2015). A brief explanation of these statistical methods is presented in the subsequent sections.

2.3.1 Linear regression

In this study, the magnitude of the trends was derived from the slope (value of 'b') of the regression line. The value of 'b', which represents the rate of change per year for the climatic variable under consideration, was multiplied by 10 to obtain the decadal change. The trends detected by the regression method were then tested for statistical significance by employing *t* test. Finally, the results obtained from the linear regression analysis were compared with those from the MK test and Sen's slope estimator.

2.3.2 Mann–Kendall rank test (MK test)

Detection of significant trends in climatic and hydrological time series is mostly facilitated by using the non-parametric MK test, which is one of the most popular trend tests. In this test, the relative values of the terms in the series X_i are used. Accordingly, the first step has to do with replacing the X_i values by relevant ranks k_i . To do so, a number (1 to N) is initially attributed to each value, and then the statistic value P is obtained as follows:

Table 1 Geographic characteristics of the rain gauge stations used in the study

<i>N</i>	Station	Latitude (N)	Longitude (E)	Altitude (m a.s.l)	Length of recorded period
1	Abelou	36°63'	53°28'	500	40
2	Abvir	37°57'	49°00'	1000	41
3	Afjeh	35°85'	51°70'	1790	38
4	Aghcheh Qayah	36°00'	48°83'	1930	34
5	Ahar	38°47'	47°00'	1345	30
6	Ahar-Tehran	35°93'	51°47'	2100	39
7	Alulak	36°42'	50°00'	1780	33
8	Amir Kabir Dam	35°93'	51°00'	1613	37
9	Ammameh-e	35°90'	51°57'	2248	32
10	Anguran	36°57'	47°60'	1600	36
11	Ardabil	38°15'	48°17'	1332	36
12	Arhan	36°30'	48°90'	2086	38
13	Armot	36°20'	50°67'	1850	39
14	Arteshabad	35°67'	49°42'	1408	41
15	Arvan	35°62'	49°18'	1850	42
16	Ashtajin	36°22'	49°75'	1316	42
17	Asmaylabad	36°22'	49°92'	1283	41
18	Azarshahr	37°78'	45°95'	1340	37
19	Babol	36°32'	52°35'	220	43
20	Baladeh	36°18'	51°78'	1875	30
21	Baraghan	36°00'	50°95'	1900	41
22	Barkala	36°63'	54°00'	1276	40
23	Bash Mahalleh	38°30'	48°82'	1559	42
24	Bastam	36°47'	54°97'	1500	54
25	Behjatabad	36°00'	50°37'	1429	43
26	Beylagan	35°83'	51°00'	1360	44
27	Bidestan	36°22'	50°00'	1310	39
28	Bon-e Kuh	35°30'	52°42'	1040	40
29	Bostanabad	37°85'	46°83'	1750	36
30	Chanasak	36°27'	50°35'	1935	39
31	Chang Almas	36°00'	49°00'	1910	39
32	Chargar	36°42'	49°00'	1922	43
33	Chubar	37°00'	49°42'	1400	30
34	Danisfahan	35°82'	49°73'	1325	36
35	Darab Kola	36°55'	53°25'	115	40
36	Darband	36°00'	50°75'	1974	38
37	Dash Tappeh	35°80'	48°86'	1830	39
38	Dashtak	35°88'	48°90'	1706	44
39	Dial Abad	36°00'	49°78'	1277	43
40	Dizan	36°27'	50°98'	1950	42
41	Doushan	35°42'	51°20'	1209	40
42	Esmaelabad	36°33'	50°00'	1300	33
43	Fasham	35°93'	51°53'	1940	38
44	Fazelabad	36°88'	54°73'	210	39
45	Firuzkuh	35°75'	52°77'	1950	41
46	Galugah	36°30'	52°62'	2000	35
47	Garmabdar	35°98'	51°62'	2500	37
48	Gatedeh	36°18'	51°00'	2600	42
49	Gelyard	36°00'	50°85'	2150	41

Table 1 (continued)

<i>N</i>	Station	Latitude (N)	Longitude (E)	Altitude (m a.s.l.)	Length of recorded period
50	Ghaz Mahale	36°78'	55°77'	55	31
51	Ghoran Talar	36°30'	52°77'	1002	41
52	Gilandeh	38°30'	48°35'	1341	33
53	Gilavan	36°77'	49°00'	1311	42
54	Gol Cheshmeh	35°52'	49°18'	2243	44
55	Harat	36°98'	50°30'	1800	42
56	Harawi	37°92'	46°48'	1920	37
57	Hashtpar	37°80'	48°90'	1999	44
58	Hoseynabad	36°72'	48°42'	1650	37
59	Jahanabad	35°88'	49°58'	1485	30
60	Jovestan	36°18'	50°88'	2003	42
61	Kakajin	36°47'	49°88'	1660	40
62	Karimabad	35°83'	50°60'	1197	38
63	Kebrit Mian	36°22'	50°25'	1473	38
64	Kelardasht	36°50'	51°17'	1380	40
65	Kenshekin	36°23'	49°58'	1597	39
66	Kharood	35°75'	49°28'	1623	43
67	Khayrabad	35°53'	53°42'	1095	40
68	Kineh Vars	36°17'	49°00'	1730	40
69	Kond Sofla	35°87'	51°65'	1950	39
70	Kooze Tooparaghi	38°00'	48°37'	1402	43
71	Kordan	35°93'	50°82'	1424	39
72	Lak	35°52'	49°78'	1934	38
73	Latyan	35°77'	51°68'	1563	41
74	Lavasan-e Bozorg	35°82'	51°75'	2260	38
75	Lay	38°00'	47°90'	2038	32
76	Liqvan	37°83'	46°43'	2200	31
77	Lowshan	36°62'	49°52'	1350	30
78	Mahmudabad	35°90'	48°92'	1714	43
79	Manjil	36°75'	49°38'	1236	43
80	Maragheh	37°40'	46°23'	1475	42
81	Marand	38°42'	46°77'	1334	31
82	Maraveh Tappeh	37°90'	55°95'	190	44
83	Mashin Khane	37°78'	48°92'	1140	43
84	Mashiran	38°67'	47°53'	705	46
85	Meyaneh	37°53'	47°35'	1480	39
86	Mihan	36°00'	49°47'	1630	44
87	Mirkoooh	38°00'	47°50'	1840	33
88	Mizuj	36°40'	50°00'	1800	41
89	Mohammadabad	36°00'	50°01'	1196	43
90	Moshampa	36°93'	47°67'	1200	36
91	Namin	38°40'	48°47'	1405	44
92	Nawar	38°00'	48°55'	2503	32
93	Nimrod	35°72'	52°65'	1820	33
94	Nir	38°00'	48°00'	1623	41
95	Nosratabad	35°53'	49°62'	1900	42
96	Nosratabad	36°00'	50°00'	1190	41
97	Nowdeh	37°00'	55°27'	1977	35
98	Nowzarabad	36°67'	54°23'	19	43

Table 1 (continued)

<i>N</i>	Station	Latitude (N)	Longitude (E)	Altitude (m a.s.l)	Length of recorded period
99	Oosta Ghasem	38°00'	48°88'	1700	41
100	Pajim	36°62'	53°72'	1250	36
101	Persianj	35°47'	49°83'	2231	40
102	Pol Almas	38°00'	48°18'	1480	45
103	Pol Arvan	35°63'	49°20'	1798	37
104	Pol Char Char	38°57'	45°72'	1350	39
105	Pol Zoghal	36°50'	51°32'	360	41
106	Polur	35°85'	52°00'	2237	40
107	Punjab	36°00'	52°27'	920	42
108	Qazvin	36°15'	50°30'	1279	53
109	Qerveh	36°00'	49°37'	1430	43
110	Qeydār	36°00'	48°58'	2000	39
111	Qoltuq	36°48'	48°07'	1800	33
112	Quzlu	35°63'	49°00'	2000	43
113	Rahimabad	35°78'	49°53'	1440	43
114	Razan	36°18'	52°17'	1240	42
115	Rig Cheshmeh	36°35'	53°17'	420	44
116	Rudak	35°85'	51°55'	1710	43
117	Rudaki	35°68'	49°88'	1467	40
118	Rudbar-e Qasran	35°87'	51°53'	1900	36
119	Rudkhan Castle	37°00'	49°27'	170	42
120	Sahlan	38°18'	46°00'	1350	33
121	Sahzab	38°00'	47°56'	1856	35
122	Saied Abad	37°98'	46°58'	1857	42
123	Sain Ghale	36°30'	49°00'	1969	43
124	Samian	38°37'	48°23'	1268	37
125	Sang Deh	36°00'	53°22'	1337	30
126	Sekranchal	36°28'	50°73'	2200	42
127	Semnan	35°35'	53°33'	1130	47
128	Sewfid Chah	36°60'	53°88'	1040	42
129	Shahrestanak	35°50'	51°00'	1056	37
130	Shahrestanak Bozorg	35°97'	51°35'	2193	38
131	Shahrood	36°25'	54°57'	1345	61
132	Shalman	37°00'	50°22'	1600	42
133	Shander	37°37'	49°00'	1968	44
134	Shanjan	38°35'	45°90'	1650	32
135	Shastkolateh	36°78'	54°37'	150	32
136	Simindasht	35°52'	52°48'	1495	36
137	Sira	36°00'	51°00'	1790	43
138	Soleyman Tange	36°25'	53°22'	1400	44
139	Sultanate	38°38'	47°67'	1485	44
140	Tabriz	38°50'	46°17'	1361	61
141	Tabriz	38°00'	46°37'	1500	31
142	Talarem	36°20'	53°25'	1200	44
143	Tangrah	37°40'	55°75'	330	34
144	Taze Konda	38°42'	47°23'	1270	30
145	Tehran	35°41'	51°19'	1190	61
146	Tekmeh Dash	37°00'	48°20'	1750	34
147	Tup Qarah	36°00'	48°75'	1850	43

Table 1 (continued)

N	Station	Latitude (N)	Longitude (E)	Altitude (m a.s.l)	Length of recorded period
148	Vatna	36°72'	53°97'	180	32
149	Zanjan	36°41'	48°29'	1663	57
150	Zereshk	36°42'	50°00'	1929	36
151	Zia Abad	35°98'	49°43'	1430	44
152	Ziaran	36°00'	50°52'	1576	44
153	Zidasht	36°17'	50°68'	1751	44
154	Zinjanab	37°85'	46°32'	2200	43

- The rank of the first value (k_1) is weighed against the ranks of the later values (from 2nd to the N th).
- The number of later values with the rank exceeding k_i is found. The number is shown by n_i .
- The rank of the second value (k_2) is weighed against the ranks of the later values and the number of later values with the rank exceeding k_i is obtained. This number is denoted by n_i .

These directions are applied for each value of the time series till k_{N-1} and its corresponding number n_{N-1} .

Using the following equation, P can be computed:

$$P = \sum_{i=1}^{N-1} n_i. \quad (1)$$

The next step involves computation of τ :

$$\tau = \frac{4P}{N(N-1)} - 1. \quad (2)$$

The value of the τ is translated into the basis of a significance test through comparing it with:

$$\tau = 0 \pm t_g \sqrt{\frac{4N+10}{9N(N-1)}}, \quad (3)$$

where t_g represents the desired probability point in terms of Gaussian normal distribution. In the present study, t_g at the 0.05 point was chosen for comparison.

2.3.3 Sequential Mann–Kendall test (SQ-MK test)

The present study used the non-parametric SQ-MK test (Sneyers 1990) to specify the change point or the approximate beginning year in significant trends. The test includes two series: progressive series $u(t)$ and backward series $u'(t)$. If these series intersect, and then set apart and exceed certain threshold values (± 1.96 for the 95% confidence level), a statistically significant trend exists. Thus, $u(t)$ should be seen as a standardized variable with zero mean and unit standard deviation and its sequential behavior revolves around the

zero level. $u(t)$ equals the values which appear in the first data point up until the last. In other words, the SQ-MK test takes into account the relative values of all terms in the time series (x_1, x_2, \dots, x_n). The test statistic is computed as follows:

- x_j annual mean time series ($j=1, \dots, n$) are evaluated with regard to x_k , ($k=1, \dots, j-1$) and the number of cases where $x_j > x_k$ are counted for each comparison and is designated by n_j .
- The test statistic is then calculated as:

$$t_j = \sum_1^j n_j. \quad (4)$$

The mean and variance are determined by:

$$e(t) = \frac{n(n-1)}{4}, \quad (5)$$

$$\text{var } t_j = \frac{j(j-1)(2j+5)}{72}. \quad (6)$$

- Finally, the sequential values of $u(t)$ are calculated using the following equation:

$$u(t) = \frac{t_j - e(t)}{\sqrt{\text{var}(t_j)}}. \quad (7)$$

In a similar procedure to $u(t)$, $u'(t)$ values are reversely calculated, starting from the end of the series. The sequential version of the MK test is an effective method to specify the beginning year of a trend. The crossing point of the forward and backward curves shows the time when a trend or change begins.

2.3.4 Sen's slope estimator

The Sen's slope estimator method was employed to specify the magnitude of the long-term trends in precipitation. With a linear trend in time series, the slope (change per

unit time) can be determined by using a simple non-parametric procedure first suggested by Sen (1968). Recently, the Sen’s slope estimator method has taken precedence over a linear regression for estimating trend slope in meteorological and hydrological studies.

The method can be expressed mathematically as follows. First, the Sen’s slope values within N pairs of data are calculated:

$$Q_i = \frac{x_j - x_k}{j - k} \quad \text{for } i = 1, \dots, N, \quad (8)$$

where x_j and x_k represent data values at times j and k ($j > k$), respectively. Sen’s estimator of slope is simply the median of these N values of Q_i . Wherever N is an odd number, the Sen’s estimator is obtained by:

$$Q_{\text{med}} = Q_{(N+1)/2}. \quad (9)$$

Wherever N is an even number, the Sen’s estimator is obtained by (Partal and Kahya 2006):

$$Q_{\text{med}} = \frac{1}{2}Q_{[N/2]} + Q_{[(N+2)/2]}. \quad (10)$$

To figure out the sum of all changes over the study period, the calculated slope can be multiplied by the number of years (here multiplied by 10 to get the decadal change).

2.3.5 Eliminating serial correlation

Prior to the statistical analysis of precipitation series, the pre-whitened test is applied to omit correlation among the series (von Storch 1995). In fact, the serial correlation significantly bears on trend detection methods (e.g., MK test) and their results. Accordingly, many recent studies have employed pre-whitened method to deal with serial correlation in meteorological parameters (e.g., Xu et al. 2010; Tabari and Hosseinzadeh Talaei 2011b; Masih et al. 2011; Zarenistanak et al. 2014b; Abghari et al. 2013; Arbabi Sabzevari et al. 2015).

The following steps are taken to identify possible statistically significant trends in the precipitation series ($x_1, x_2, x_3, \dots, x_n$).

- Step 1* Find lag-1 serial correlation coefficient (represented by r_1)
- Step 2* If r_1 is not significant at the 5% level, the original data of the time series must be tested
- Step 3* If the calculated r_1 is significant, first the pre-whitened test is performed rather than statistical tests. Pre-whitened test is performed via this formula: $(x_2 - r_1x_1, x_3 - r_1x_2, \dots, x_n - r_1x_{n-1})$ (Partal and Kahya 2006).

2.3.6 Coefficient of variation (CV)

To understand the variability in precipitation, CV, a statistical measure of the dispersion of data points in a data series around the mean was calculated by the following formula:

$$\text{Coefficient of variation} = \frac{S}{\bar{x}} * 100, \quad (11)$$

where \bar{x} is the average of rain gauge stations and S is the standard deviation for each station. In other words, the coefficient of variation represents the ratio of the standard deviation to the mean and is a useful tool for comparing the degree of variation from one data series to another, even if the means are drastically different from each other.

2.4 Model description

In this study, the outputs from three GCMs were used under two scenarios (i.e., RCP4.5 and RCP8.5) for precipitation projections in the north of Iran. The coupled climate models, whose data were available, are listed with key references in Table 2. Using Gordess and Matlab software, data points were extracted from global data, while the GIS application was employed to locate the coordinates. Afterward, a mean value of the points was processed and utilized. The historical simulations were integrated from 1980 to 2000, and the projections for both RCP4.5 and RCP8.5 were analyzed from 2000 to 2100. RCP4.5 is a stabilization scenario in which the total radiative forcing is stabilized before 2100, without overshooting. It uses a range of new technologies and strategies for reducing greenhouse gas emissions (GHGs). RCP4.5 and RCP8.5 indicate a concentration pathway that results in a radiative forcing of ~ 4.5 and $\sim 8.5 \text{ W m}^{-2}$ in

Table 2 Climate models and their key references participating in the CMIP5

Models	Institution	Institution ID	Country	Latitude	Longitude	Key references
GFDL-CM3	Geophysical Fluid Dynamics Laboratory	GFDL	USA	2.00	2.50	Delworth et al. (2006)
HadGEM2-AO	National Institute of Meteorological Research/Korea Meteorological Administration	NIMR/KMA	Korea	1.25	1.875	Baek et al. (2013)
MPI-ESM-MR	Max Planck Institute Earth System Model	MPI-M	Germany	1.8653	1.875	Giorgetta et al. (2013)

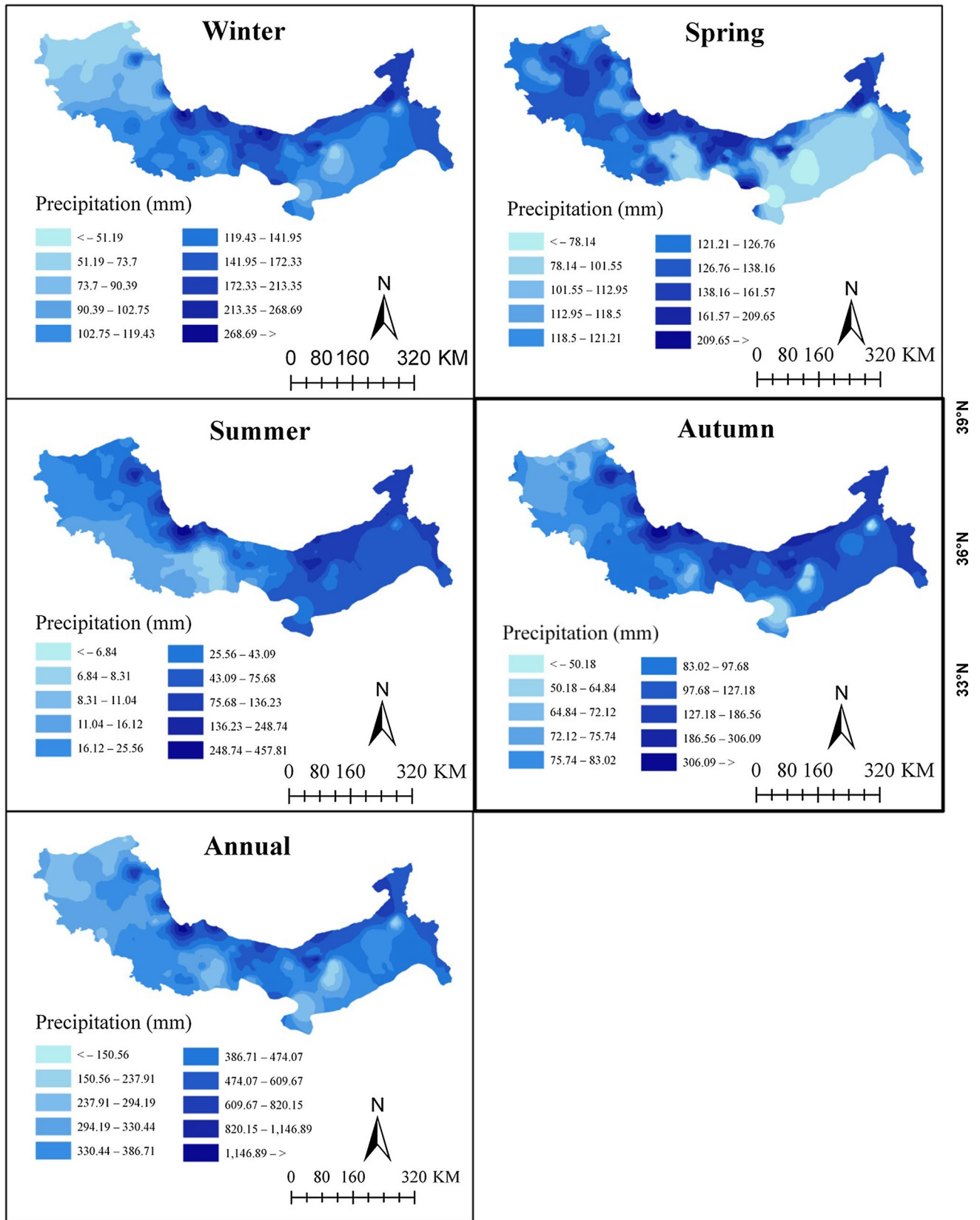


Fig. 2 Annual and seasonal precipitation zones

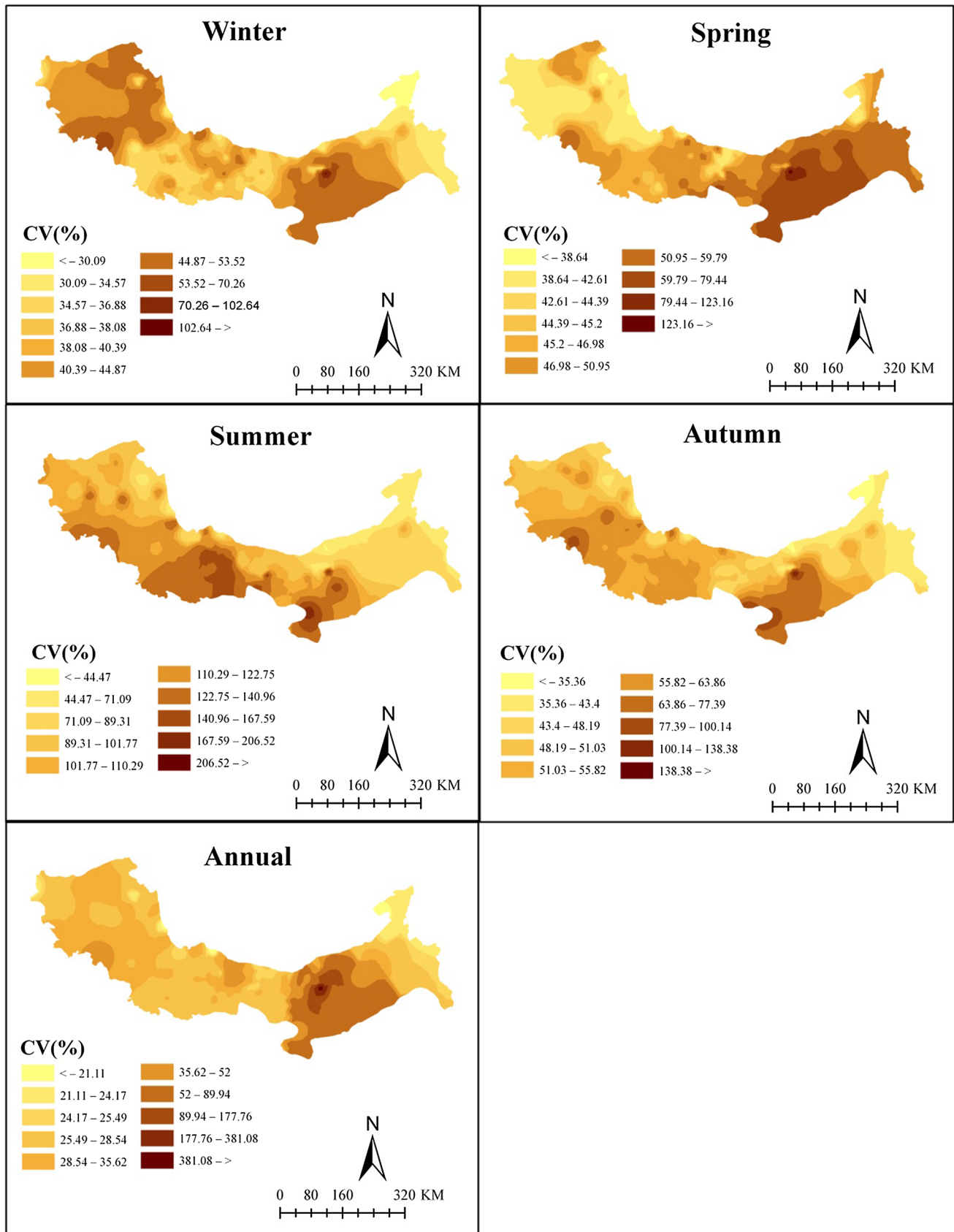


Fig. 3 Spatial pattern of coefficient of variation of annual and seasonal precipitation zones

Table 3 Results of the significant lag-1 serial correlation coefficient for annual and seasonal precipitation series

	Positive	Negative
Winter	26	7
Spring	23	9
Summer	13	8
Autumn	17	12
Annual	32	14

2010, respectively. RCP 8.5 is characterized by increasing GHGs over time, which leads to higher GHG concentrations and is related to preindustrial conditions (Taylor et al. 2009; Wei and Bao 2012).

3 Results and discussion

3.1 Trend analysis

Annual and seasonal precipitation and CV zones for the period 1950–2014 are depicted in Figs. 2 and 3, respectively. The mean annual precipitation for the study period was 440 mm. Ten stations from the west of the Caspian Sea coasts received annual precipitation more than 1000 mm. The mean average seasonal precipitation from 1950 to 2014 were 136, 131, 51 and 126 mm in winter, spring, summer and autumn, respectively. CV was computed for all stations

to investigate the spatial pattern of precipitation variability over the study area. In annual CV zones, most of the stations located in the east of the study area indicated the largest CV values where the precipitation amount was low (Fig. 3). In addition, the winter and summer seasons showed the lowest and highest CV, respectively. The average CV for annual precipitation is 33%, for winter 32%, for spring 47%, for summer 105% and for autumn 51%.

A preliminary analysis showed that the majority of the precipitation time series had no significant lag-1 serial correlation coefficient (Table 3). The highest number of significant serial correlation was observed in the annual series.

Figure 4 shows the percentage of stations with significant trends in the annual and seasonal precipitation time series for the period 1950–2014. Both positive and negative trends were identified by the linear regression, the MK test, the SQ-MK test and the Sen's slope estimator in the annual and seasonal precipitation series. Nevertheless, most of the trends were insignificant at the 95% confidence level. Based on the results of the linear regression analysis, spatial distribution maps for precipitation significant changes (in mm/decade) were prepared as presented in Fig. 5. In the annual precipitation series, on average 11% of the stations showed a significant positive trend and 20% showed a significant negative trend. Spatial distribution of annual precipitation trends showed negative tendencies in the central parts of the study area with rates ranging between -20 and -100 mm/decade (Fig. 5). Five stations showed a significant positive

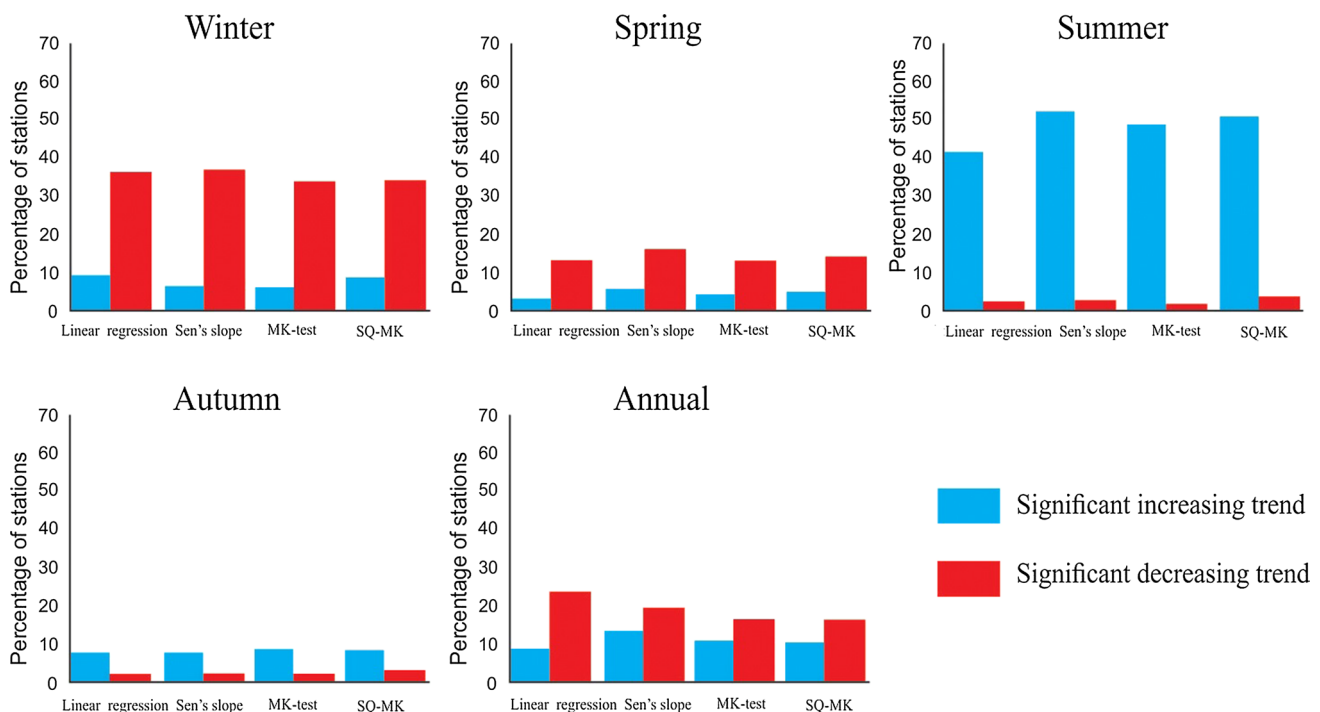


Fig. 4 Percentage of stations with significant trends at the 95% confidence level by linear regression, SQ-MK test, MK test and Sen's slope estimator for annual and seasonal precipitation series

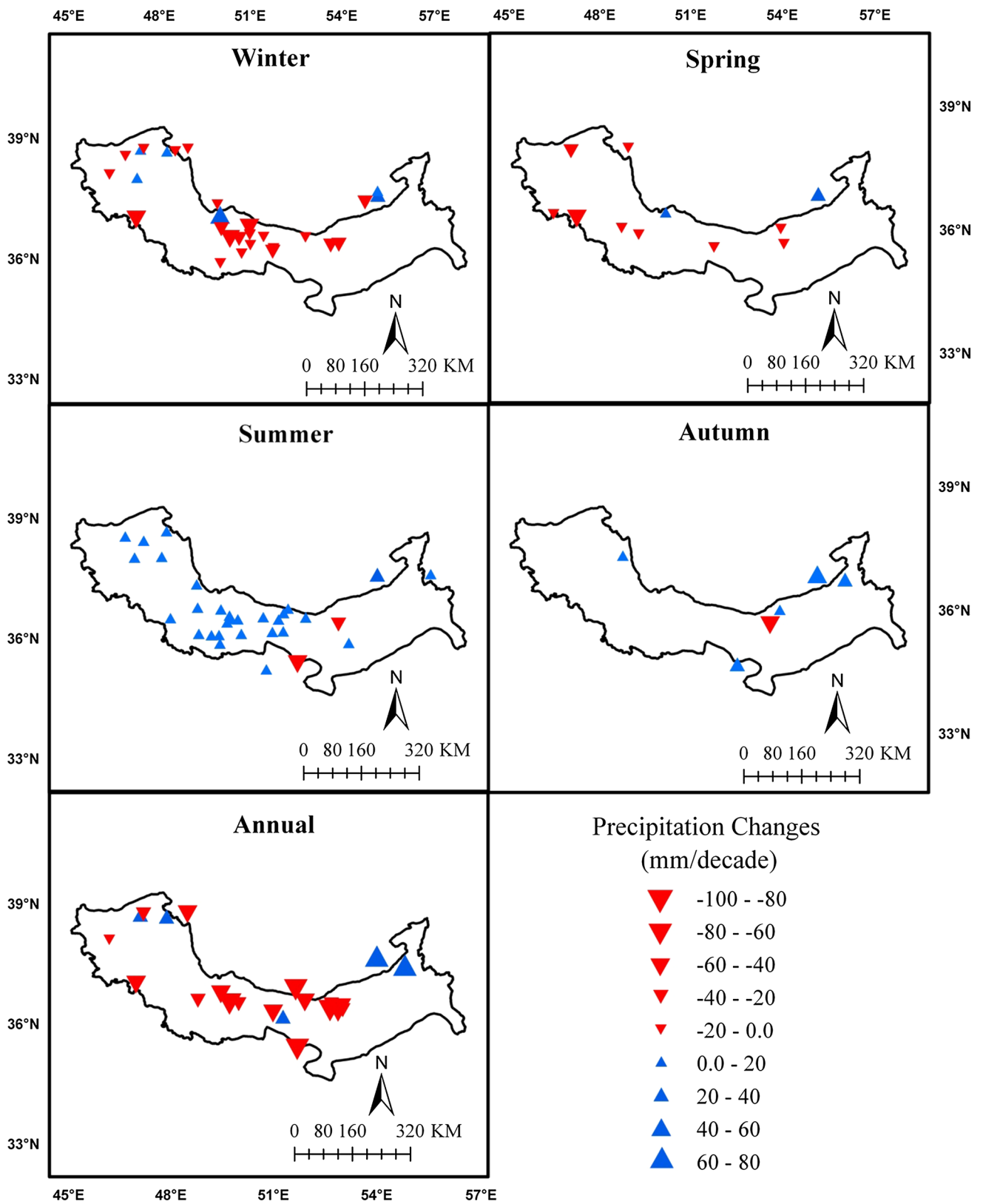


Fig. 5 Significant trends (mm/decade) in annual and seasonal precipitation

Table 4 Values from stations recording significant mutation points (in percent)

	1950s		1960s		1970s		1980s		1990s		2000s	
	<i>P</i>	<i>N</i>	<i>P</i>	<i>N</i>	<i>P</i>	<i>N</i>	<i>P</i>	<i>N</i>	<i>P</i>	<i>N</i>	<i>P</i>	<i>N</i>
Winter	0	0	0	3	87	66	10	20	3	10	0	1
Spring	0	0	8	17	52	40	25	22	13	21	2	0
Summer	0	0	12	0	56	100	34	0	0	0	0	0
Autumn	0	0	0	0	100	100	0	0	0	0	0	0
Annual	0	0	7	17	87	70	3	10	3	3	0	0

P positive, *N* negation

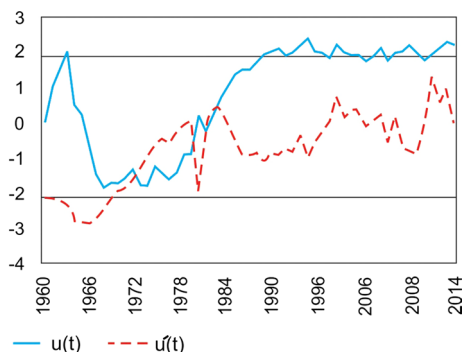


Fig. 6 Graphical illustration of the series $u(t)$ (solid line) and backward series $u'(t)$ (dashed line) of the SQ-MK test for annual precipitation series observed at Bastam station

trend for annual precipitation with rates ranging between 40 and 60 mm/decade. Shifteh Some'e et al. (2012) reported that over the 1950–2006 period, a negative trend in annual precipitation occurred at 79% of Iranian stations, while only three stations had a significant negative trend at the 95% confidence level. In addition, Tabari et al. (2011) found insignificant negative trends in the annual precipitation series at the majority of the Iranian stations.

For all the selected stations, the linear regression analysis, the MK test, the SQ-MK test and the Sen's slope estimator were also applied to detect the trends of the seasonal

precipitation time series during 1950–2014 (Figs. 4, 5). As shown in Fig. 4, the majority of the trends in the seasonal series occurred in winter (negative) and summer (positive). Based on the results of the statistical tests, the significant negative trends in the winter precipitation series were found at 35% of the stations (Fig. 4). 21 stations with significant negative trends are located in the west and central parts of the study area with a trend magnitude ranging between -20 and -100 mm/decade (Fig. 5). The stations with the altitudes higher than 1500 m show significant negative trends during winter, especially in case of the Central Alborz Range (Fig. 5). A review of the data revealed that snowfall amount was decreased, probably due to less snow cover which itself invites further studies. Five stations revealed a significant positive trend during winter with a slope range between 6 and 57 mm/decade. Spring precipitation mainly decreased in the western parts of the study area characterized by six stations. Significant positive trends were found only at Vatana and Lowshan stations with rates of 30 and 15 mm/decade, respectively. Summer precipitation increased more during the study period as compared to the other seasons. The results of linear regression analysis, MK test and Sen's slope estimator showed 47, 60 and 56% of the stations having a significant positive trend with increasing trend rates of 5 and 40 mm/decade, respectively. The precipitation systems that move to Iran via the Mediterranean Sea are stopped or diminished during summer, mainly because of the presence

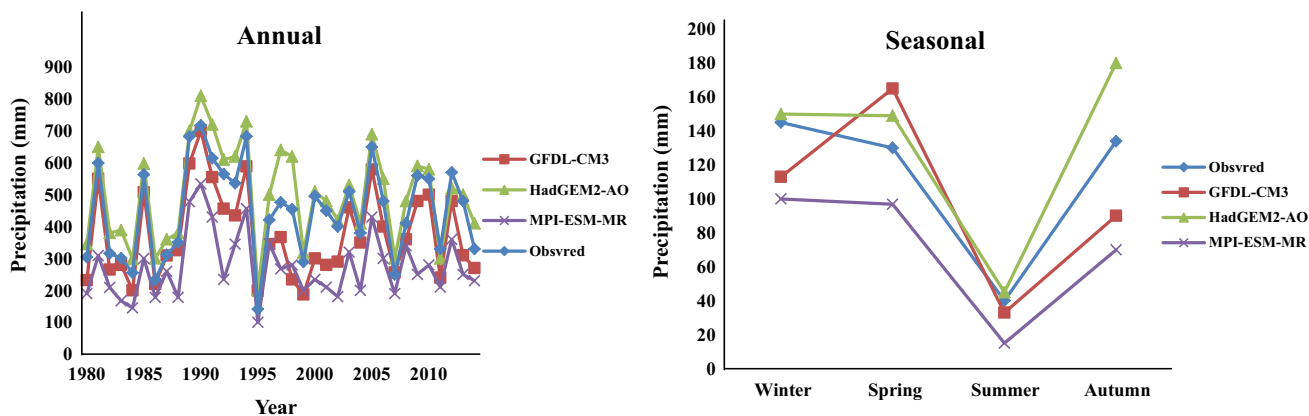


Fig. 7 Average of the observed precipitation and the simulations by the three models from 1980 to 2014

of the subtropical high, giving way to the regional precipitation systems. During this season, most of the rain gauge stations installed in the Central Alborz Range and also in the foothills facing the Caspian Sea coasts indicate significant positive trends (22 stations). Mountains and heights in the Central Alborz Range are close to the sea, allowing increasingly humidity entrance to the region, while temperature and vaporization escalate, leading to the emergence of convectional rainfalls. Mir Kuh, Harawi, Bostanabad, Sahzab and Sultanate stations situated in the western parts of the study area show significant positive trends, a fact explained by regional factors especially topographic features. These stations lie in valleys that carry humidity from the Caspian Sea. Sقانfar Qur'an and Ammameh-e in the east of the study area, located at the bottom of foothills against the sea, showed significant negative trends with rates of -28 and -42 mm/decade, respectively.

As shown in Fig. 4, autumn precipitation was more stable than the other seasons. Now Deh, Vatana, Soleyman Tangeh, Mohammad Deh and Ammameh-e showed significant positive trends with rates of 27, 52, 13, 8 and 36 mm/decade, respectively. Only Galugah station showed a significant negative trend at the rate of -31 mm/decade. Hosseinzadeh Talaee (2014) found an insignificant trend in the annual and seasonal rainfall series at the majority of the considered stations over Iran.

It was revealed that those stations with significant positive trends in winter, autumn and spring are mostly either inside

or in the vicinity of towns (Now Deh, Vatana, Soleyman Tangeh, Mohammad Deh, Ammameh-e Lowshan). Thanks to urban expansions in Iran, especially since the 1970s, and migration of populations from countryside to cities, urban areas have come to occupy more lands, enveloping the stations that used to lie outside city limits. In fact, the positive rainfall trends are influenced by urban microclimate. It should be noted these speculations are authorial.

Following the SQ-MK test, a graphical analysis using $u(t)$ and $u'(t)$ statistics was performed for the annual and seasonal precipitation series at 154 study stations. In this way, the onset of the change in the time series is detected by pinpointing the intersection point of the curves. The positive or negative trend for each station is also determined by analyzing the plots as well as the point of change in the mutation point. The results of the SQ-MK test for the period 1951–2014 reveal a statistically significant mutation point in the annual and seasonal precipitation time series in the 1970s at most of rain gauge stations (Table 4). All mutation points (either positive or negative) in the autumn series occurred in the 1970s. Similarly, all negative mutation points in the summer series occurred in the 1970s. Following the 1970s, most of the mutation points lie in the 1980s. An illustrative example is shown in Fig. 6, which clearly demonstrates a mutation point in 1973 in the total annual precipitation time series of Bastam. These findings are in good agreement with the results of Nazemosadat et al. (2006), who found a significant mutation point in or around the mid-1970s over the northern

Table 5 Precipitation changes (%) for the period 1981–2100

	RCP4.5					RCP8.5				
	Winter	Spring	Summer	Autumn	Annual	Winter	Spring	Summer	Autumn	Annual
GFDL-CM3	4.60	-5.31	-53.72	1.25	-4.73	-16.17	-6.68	-63.19	-12.58	-14.95
HadGEM2-AO	13.72	-10.46	12.10	4.35	3.56	18.59	-14.89	-11.08	-79.86	5.21
MPI-ESM-MR	-5.84	-28.76	-128.04	5.32	-12.36	-12.10	-35.55	-70.28	24.09	-14.05

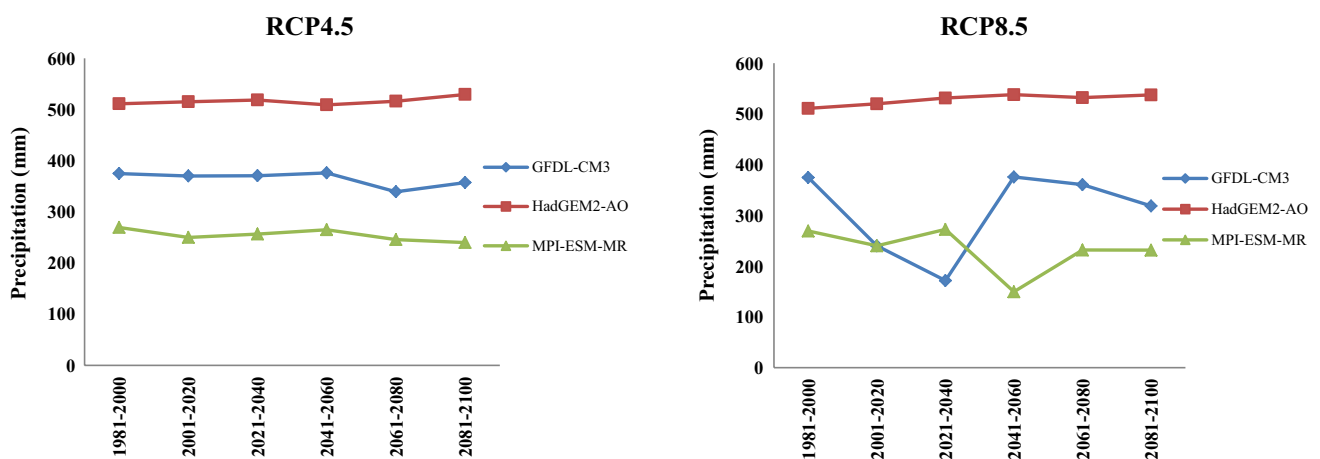


Fig. 8 Projections for annual precipitation under the RCP 4.5 and RCP 8.5 scenarios

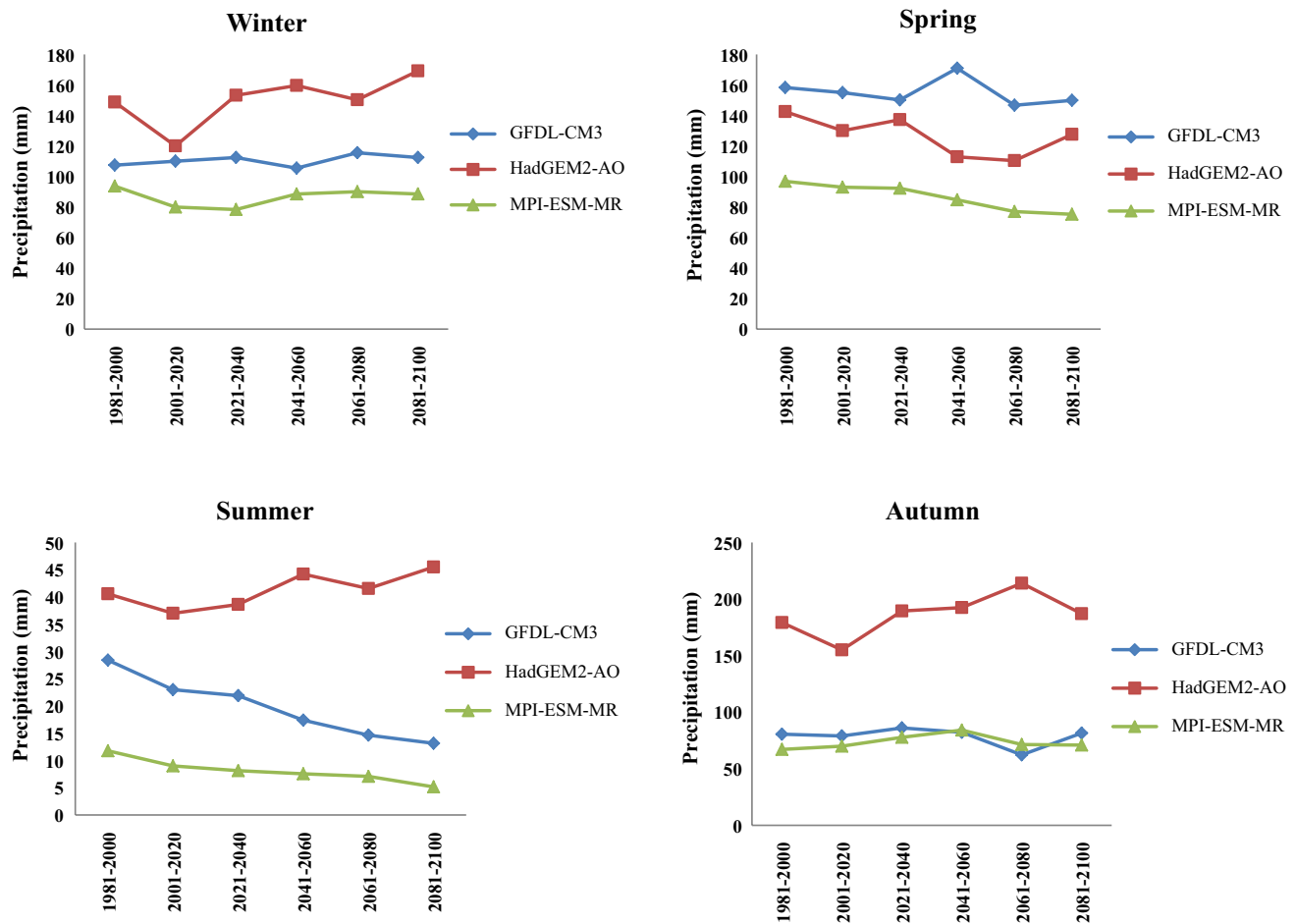


Fig. 9 Projections for seasonal precipitation series under the RCP 4.5 scenario

parts of Iran. He reported that the mid-1970s is the most probable change point year in the time series of the Southern Oscillation Index (SOI) data for the period 1951–1999 over Iran. Consistent with this finding, precipitation data from the northern parts of Iran have also shown significant change years in or around the mid-1970s. Molavi-Arabshahi et al. (2016) revealed that during 1996–2010 precipitation variations over the southwest coast of the Caspian Sea show strong connections with ENSO and weaker ones with NAO (North Atlantic Oscillation). The trends of precipitation during this period are diverse, but display mostly a weak decrease. Besides ENSO, Madden Jullian Oscillation (MJO) also plays a role in Iran in terms of precipitation variability, as suggested by Nazemosadat and GHaed Amini AsadAbadi (2010) and Nazemosadat and Shahgholian (2017).

For annual precipitation series of the period 1950–2014, most of the stations under study show insignificant trends, a result very much in line with what previous research has found either in Iran or certain parts of it (e.g., Tabari and Hosseinzadeh Talaei 2011a; Moazed et al. 2012; Shifteh Some'e et al. 2012; Razinei et al. 2014; Khalili et al. 2014).

For the seasonal series, winter shows the greatest number of significant negative trend, while summer shows the greatest significant positive trend. This matches the results reported by Shifteh Some'e et al. (2012), who found a decrease in winter precipitation amount for the northern part of Iran. An increasing trend in summer was also noted by Javari (2016) in the west and north of Iran for the period 1975–2014. In addition, Asakereh (2016) found a small increase in summer precipitation in the northwest of Iran.

3.2 Precipitation projections

In this study, precipitation historical (1980–2000) and future (2000–2100) runs of three CMIP5 global climate models (GFDL-CM3, HadGEM2-AO and MPI-ESM-MR) were employed. The projection was based on two representative concentration pathways (RCP4.5 and RCP8.5). Figure 7 depicts a comparison between the observed seasonal precipitation series (mm) and the simulations from each model for the period 1981–2014 to evaluate the accuracy of the

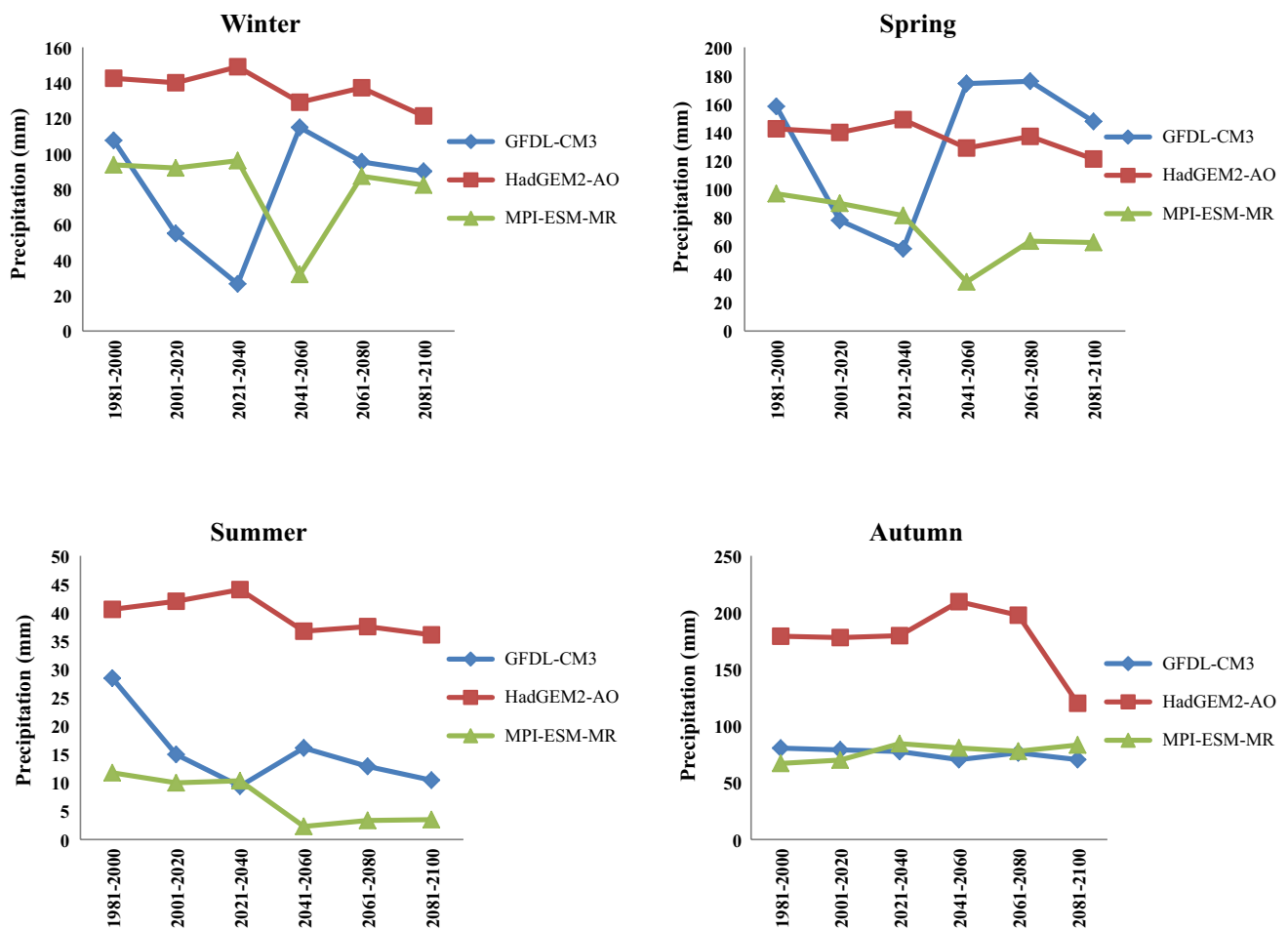


Fig. 10 Projections for seasonal precipitation series under the RCP 8.5 scenario

model outputs. Based on the observed data, the models can be classified into two categories: GFDL-CM3 and MPI-ESM-MR models underestimated annual precipitation, while HadGEM2-AO model overestimated it.

The range of precipitation changes is presented in Table 5. The precipitation projections do not indicate substantial future precipitation changes except in the summer. Most of the models under both scenarios showed a precipitation decrease by the end of the twenty-first century. Figure 8 shows future projections of annual mean precipitation. The results of the GFDL-CM3 model showed that precipitation may decrease by -4.7 and -14.95% under RCP4.5 and RCP8.5, respectively. The results of the HadGEM2-AO model showed that precipitation may increase by 3.5% by 2100 based on the RCP4.5 scenario. However, the projections for the RCP8.5 scenario indicated that precipitation may increase by 5.2% by 2100. The MPI-ESM-MR model projected precipitation decreases of -12.36 and -14.05% by 2100 based on the RCP4.5 and RCP8.5 scenarios, respectively. Roshan et al. (2012) reported annual precipitation increases of 25.19 and 26.4% for 2025 and 2050 compared

to 2005, respectively. Babaeian et al. (2013) also found that annual mean precipitation over the southeast of the Caspian Sea, in the south of the Zagros Mountains and northwest and southeast provinces of Iran, will decrease by 0.1–0.2 mm/day under the A2 and B2 scenarios compared to 1961–1990.

The results of seasonal precipitation projections using three models under the RCP4.5 and RCP8.5 scenarios for the periods 1981–2000, 2001–2020, 2021–2040, 2041–2060, 2061–2080 and 2081–2100 are depicted in Figs. 9 and 10, respectively. In the seasonal time series, larger precipitation changes may happen in the summer season under both scenarios. The time series of spring precipitation showed a decrease by all three models under both scenarios (Table 5). As compared with the base period, precipitation may decrease in summer under the RCP8.5 scenario according to all the models. Under the RCP4.5 scenario, precipitation may increase in autumn according to all the models. The precipitation changes for the twenty-first century are not uniform. No clear pattern in precipitation changes is evident during any season, as can be seen in Figs. 9 and 10. This may be due to the complexity in interpreting precipitation

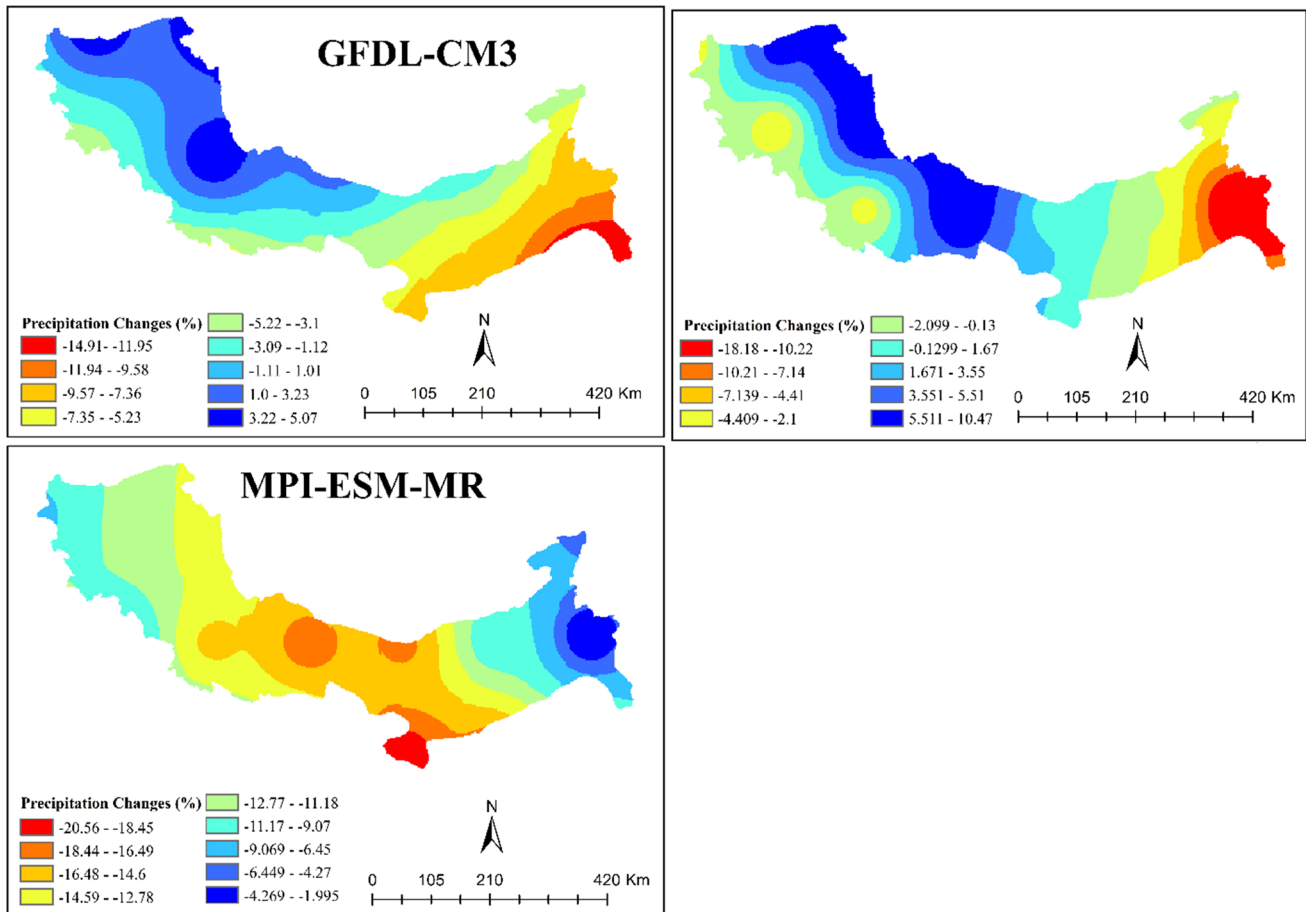


Fig. 11 Projected annual precipitation changes between the late twentieth century (1981–2000) and the late twenty-first century (2081–2100) under the RCP 4.5 emission scenario

projections, since different models often do not agree on whether precipitation will increase or decrease at a specific location and agree even less on the magnitude of that change (Agarwal et al. 2014).

Figures 11 and 12 illustrate the changes in annual precipitation between 1981–2000 and 2081–2100 over the study area under both scenarios. Precipitation may increase in the northwest of the study area up to 3.2% as compared to 1981–2000. Precipitation may decrease from the west to the east of the study area under the RCP 4.5 scenario (Fig. 11). The GFDL-CM3 model showed a precipitation decrease in the entire study area under the RCP 8.5 scenario at the rate between -9 and -11% (Fig. 12). According to the HadGEM2-AO model, under the RCP4.5 scenario, precipitation may increase in the northwest of the study area, while a decrease was projected for the southeast of the study area as compared to the base period (Fig. 11). Under the RCP8.5 scenario, precipitation may increase in the central part of the study area and decrease in the west and east regions (Fig. 12). The MPI-ESM-MR model, under both scenarios,

projected a precipitation decrease, for the whole study area with larger decrease in the central part (Figs. 11 and 12).

4 Conclusions

In the present study, a statistical trend analysis and projections of annual and seasonal precipitation were performed in the Alborz Mountains area. The linear regression, the MK test, the SQ-MK test and the Sen's slope estimator were used for trend analysis at 154 stations in the Alborz Mountains area for the period 1950–2014. To evaluate the homogeneity of the precipitation data, the Pettitt's and Buishand range, the standard normal homogeneity and the standard normal homogeneity by Alexandersson and Moberg tests were applied. Furthermore, pre-whitening approach was applied to eliminate the effect of serial correlation on the MK test. The precipitation projections from 1980 to 2100 were derived from three CMIP5 datasets under the RCP 4.5 and RCP 8.5 scenarios. The results of the homogeneity test showed that the precipitation series were not affected.

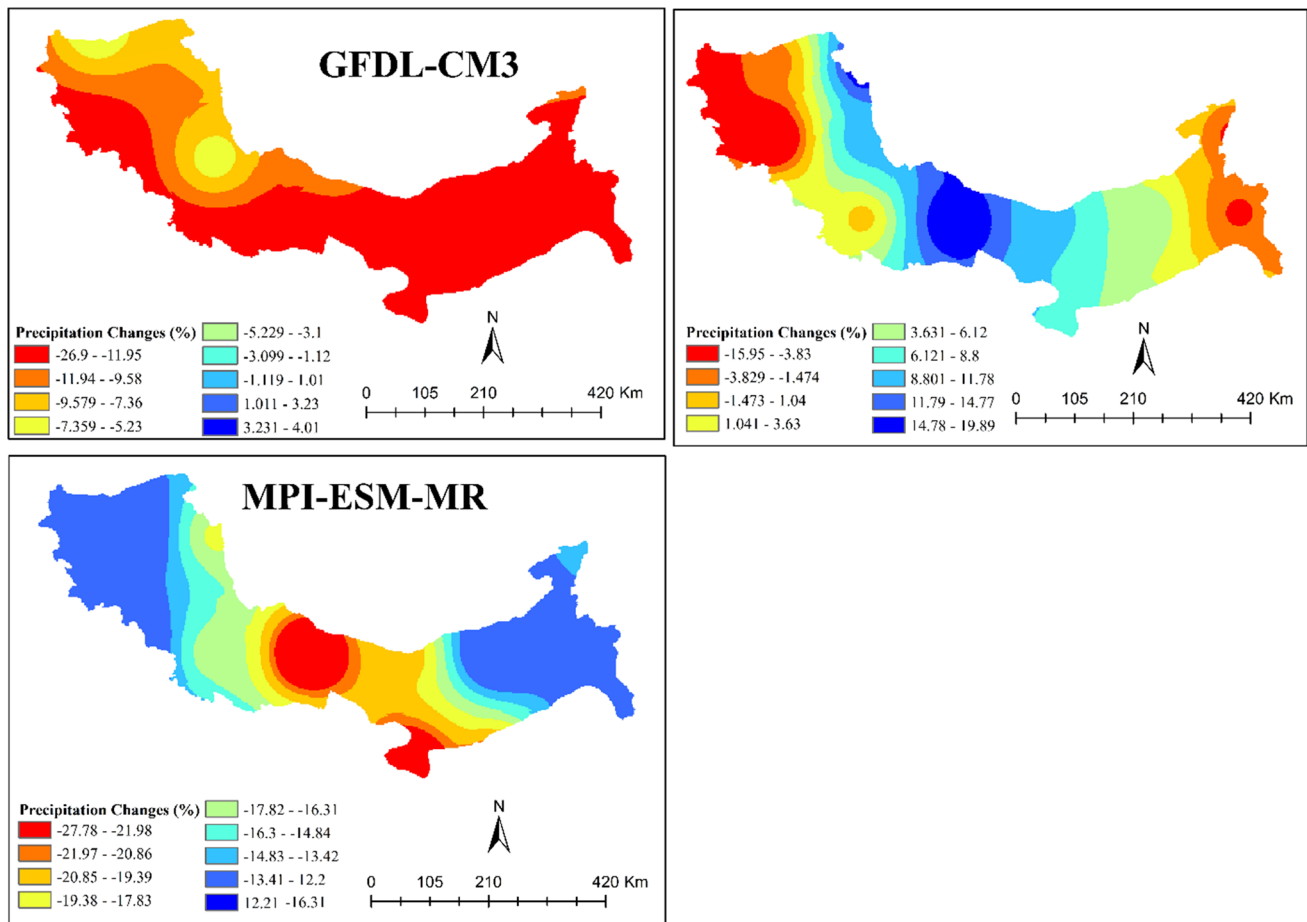


Fig. 12 Projected annual precipitation changes between the late twentieth century (1981–2000) and the late twenty-first century (2081–2100) under the RCP 8.5 emission scenario

The results of pre-whitening showed that precipitation data were serially correlated showing the independency of the data. The results of the trend analysis indicated insignificant trends in annual and seasonal precipitation at most of the stations considered. Furthermore, at the seasonal level, the highest number of stations with significant negative trends in precipitation occurred in winter, while positive significant trends were detected in summer precipitation. The results of the SQ-MK test show that most of the significant mutation points in annual and seasonal precipitation series began in the 1970s. The previous research indicated that precipitation variability in the study area significantly influenced by the ENSO phenomenon.

Based on the results, CMIP5 can also simulate the precipitation variability in the Alborz Mountains area during the period 1980–2100. The projected precipitation changes showed that precipitation may decrease according to most of the models under the RCP 4.5 and RCP 8.5 scenarios, but the decrease may not be large except in summer in 2100.

Due to the distance between the spots, their height, and the validity of output, the model precipitation simulations

are less reliable in mountainous regions than other areas. However, experts and policy makers can hugely benefit from the results in drawing more accurate plans for water resource management in arid and semi-arid countries such as Iran. Results of climate changes in Iran affect not only precipitation and temperature, but also drought, successive hurricanes, vaporization, humidity and particularly agriculture. Yet, all these repercussions must be taken into account to assess their influence on the economy, environment, water resources and most importantly on food security in the twenty-first century. In this way, policy makers can better prepare for possible negative outcomes that may challenge people’s lives.

Acknowledgements The author is thankful to the Islamic Republic of Iran Meteorological Organization, Iranian Water Resources Management Organization, Ministry of Energy for providing necessary data required for the study. I also acknowledge the modeling groups for providing their data for analysis, the PCMDI, Lawrence Livermore National Laboratory, USA, for collecting and archiving the model output and for providing necessary data required for the study. The author is also grateful to Dr. R. H. Kripalani and Dr. Preethi from the Indian

Institute of Tropical Meteorology, Pune, India, for their suggestions on projection analysis. Also, the author would like to thank the anonymous reviewers for their comments and suggestions which have contributed to improve the manuscript.

References

- Abghari H, Tabari H, Hosseinzadeh Talae P (2013) River flow trends in the west of Iran during the past 40 years: impact of precipitation variability. *Glob Planet Chang* 101:52–60
- Agarwal A, Babel MS, Maskey S (2014) Analysis of future precipitation in the Koshi river basin. *Nepal J Hydrol* 513:422–434
- Alexandersson H (1986) A homogeneity test applied to precipitation data. *Int J Climatol* 6:661–675
- Alexandersson H, Moberg A (1997) Homogenization of Swedish temperature data. Part I: homogeneity test for linear trends. *Int J Climatol* 17:25–34
- Alijani B (1995) Climate of Iran. University of PayameNour, Tehran
- Alizadeh A, Keshavarz A (2005) Cwater use in Iran. *Water conservation, reuse, and recycling: proceedings of an Iranian American Workshop*, pp 94–105
- Amiri J, Eslamian S (2010) Investigation of climate change in Iran. *Environ Sci Technol* 3:208–216
- Arbabi Sabzevari A, Zarenistanak M, Tabari H, Moghimi S (2015) Evaluation of precipitation and river discharge variations over southwestern Iran during recent decades. *J Earth Syst Sci* 124(2):335–352
- Asakereh H (2016) Trends in monthly precipitation over the northwest of Iran (NWI). *Theor Appl Climatol*. <https://doi.org/10.1007/s00704-016-1893-8>
- Ay M, Kisi O (2015) Investigation of trend analysis of monthly total precipitation by an innovative method. *Theor Appl Climatol* 120:617–629
- Babaeian I, Najafi Z, ZabolAbbasi F, Habibi Nokhandan M, Adab H, Malbosi SH (2013) Climate change assessment over Iran during 2010–2100 by using statistical downscaling of ECHO-G model. *Geogr Dev* 6(6):135–152
- Babaeiana I, Modiriana R, Karimiana M, Zarghamib M (2015) Simulation of climate change in Iran during 2071–2100 using PRE-CIS regional climate modelling system. *Desert* 20(2):123–134
- Baek H, Lee J, Lee H, Hyun Y, Cho C, Kwon W, Marzin C, Gan S, Kim M, Choi D, LeeJ Lee J, Boo K, Kang H, Byun Y (2013) Climate change in the 21st century simulated by HadGEM2-AO under representative concentration pathways, Asia–Pacific. *J Atmos Sci* 49:603–618
- Buishand TA (1982) Some methods for testing the homogeneity of rainfall records. *J Hydrol* 58:11–27
- Chandniha SK, Meshram S, Adamowski JF, Meshram C (2016) Trend analysis of precipitation in Jharkhand state. *Theor Appl Climatol*, India. <https://doi.org/10.1007/s00704-016-1875-x>
- Chen FH, Huang W, Jin LY et al (2011) Spatio-temporal precipitation variations in the arid Central Asia in the context of global warming. *Sci China Earth Sci*. <https://doi.org/10.1007/s11430-011-4333-8>
- Delju AH, Ceylan A, Piguat E, Rebetez M (2013) Observed climate variability and change in Urmia lake basin, Iran. *Theor Appl Climatol* 111:285–296
- Delworth TL, Broccoli AJ, Rosati A, Stouffer RJ et al (2006) GFDL's CM2 global coupled climate models part 1 formulation and simulation characteristics. *Climate* 19:643–674
- Deng H, Luo Y, Yao Y, Liu C (2013) Spring and summer precipitation changes from 1880 to 2011 and the future projections from CMIP5 models in the Yangtze river basin, China. *Quat Int* 304:95–106
- Dhorde AG, Zarenistanak M, Kripalani RH, Preethi B (2014) Precipitation analysis over southwest Iran: trends and projections. *Meteorol Atmos Phys* 124:205–216
- Dinpashoh Y, Jhajarha D, Fakheri-Fard A, Singh VP, Kahya E (2011) Trends in reference crop evapotranspiration over Iran. *J Hydrol* 399(3):422–433
- Eccel E, Tomozeiu R (2015) Increasing resolution of climate assessment and projection of temperature and precipitation in an alpine area. *Theor Appl Climatol* 120:479–493
- Farhangi M, Kholghi M, Chavoshian S (2016) Rainfall trend analysis of hydrological subbasins in Western Iran. *J Irrig Drain Eng*. [https://doi.org/10.1061/\(asce\)ir.1943-4774.0001040.05016004](https://doi.org/10.1061/(asce)ir.1943-4774.0001040.05016004)
- Feizi V, Mollashahi M, Frajzadeh M, Azizi G (2014) Spatial and temporal trend analysis of temperature and precipitation in Iran. *Eco-persia* 2(4):727–742
- Giorgetta M et al. (2013) CMIP5 simulations of the Max Planck Institute for Meteorology (MPI-M) based on the MPI-ESM-LR model: the amip future experiment, served by Esgf. Wdcc at Dkrz <https://doi.org/10.1594/wdcc/cmip5.mxelaf>
- Hanif M, Khan AH, Adnan S (2013) Latitudinal precipitation characteristics and trends in Pakistan. *J Hydrol* 492:266–272
- Hosseinzadeh Talae P (2014) Iranian rainfall series analysis by means of nonparametric tests. *Theor Appl Climatol* 116:597–607
- Hu C, Xu Y, Han L, Yang L, Xu G (2016) Long-term trends in daily precipitation over the Yangtze river delta region during 1960–2012, Eastern China. *Theor Appl Climatol* 125:131–147
- IPCC (2014) In: Barros VR, Field CB, Dokken DJ, Mastrandrea MD, Mach KJ, Bilir TE, Chatterjee M, Ebi KL, Estrada YO, Genova RC, Girma B, Kissel ES, Levy AN, MacCracken S, Mastrandrea PR, White LL (eds) *Climate change 2014: impacts, adaptation, and vulnerability. Part B: regional aspects. Contribution of Working Group II to the fifth assessment report of the intergovernmental panel on climate change*. Cambridge University Press, Cambridge
- Jafari M (2012) Adaptation of global climate change projections for local level application: case study, special forest ecosystem, Astara. *Iran J Nat Resour Res* 1:12–23
- Javari M (2016) Trend and homogeneity analysis of precipitation in Iran. *Climate*. <https://doi.org/10.3390/cli4030044>
- Jiang R, Gan TY, Xie J, Wang N, Kuo C (2015) Historical and potential changes of precipitation and temperature of Alberta subjected to climate change impact: 1900–2100. *Theor Appl Climatol*. <https://doi.org/10.1007/s00704-015-1664-y>
- Khalili K, Tahrudi MN, Khanmohammadi N (2014) Trend analysis of precipitation in recent two decades over Iran. *J Appl Environ Biol Sci* 4(1):5–10
- Kousari Ekhtesasi MR, Tazeh M, Saremi Naeini MA, Asadi Zarch MA (2011) An investigation of the Iranian climatic changes by considering the precipitation, temperature, and relative humidity parameters. *Theor Appl Climatol* 103:321–335
- Liu L, Hong Y, Hocker JE, Shafer MA, Carter LM, Gourley JJ, Bednarczyk CN, Yong B, Adhikari P (2012) Analyzing projected changes and trends of temperature and precipitation in the southern USA from 16 downscaled global climate models. *Theor Appl Climatol* 109:345–360
- Martinez CJ, Maleski JJ, Miller MF (2012) Trends in precipitation and temperature in Florida, USA. *J Hydrol* 452(453):259–281
- Masih I, Uhlenbrook S, Maskey S, Smakhtin V (2011) Stream flow trends and climate linkages in the Zagros Mountains, Iran. *Clim Chang* 104(2):317–338
- Meshram SG, Singh VP, Meshram C (2016) Long-term trend and variability of precipitation in Chhattisgarh state, India. *Theor Appl Climatol*. <https://doi.org/10.1007/s00704-016-1804-z>

- Moazed H, Salarijazi M, Moradzadeh M, Soleymani S (2012) Changes in rainfall characteristics in Southwestern Iran. *Afr J Agric Res* 7(18):2835–2843
- Molavi-Arabshahi M, Arpeb K, Leroy S (2016) Precipitation and temperature of the southwest Caspian Sea region during the last 55 years: their trends and teleconnections with large-scale atmospheric phenomena. *Int J Climatol* 36:2156–2172
- Nazemosadat MJ (2001) The impact of the Caspian Sea surface temperature on rainfall over northern parts of Iran. In: Book of abstracts, 2nd National Conference of the Royal Meteorological Society, 12–14 September, England
- Nazemosadat MJ, GHaed Amini AsadAbadi H (2010) The influence of Madden-Julian oscillation on occurrence of February to April extreme precipitation (flood and drought) in Fars Province. *J Water Soil Sci* 12(46):477–489
- Nazemosadat MJ, Ghasemi AR (2004) Quantifying the ENSO related shifts in the intensity and probability of drought and wet periods in Iran. *J Clim* 17(20):4005–4018
- Nazemosadat MJ, Shahgholian K (2017) Heavy precipitation in the southwest of Iran: association with the Madden-Julian oscillation and synoptic scale analysis. *Clim Dyn* 49:3091–3109
- Nazemosadat MJ, Samani N, Barry DA, Molaii Niko M (2006) ENSO forcing on climate change in Iran: precipitation analyses. *Iran J Sci Technol Trans B Eng* 30(B4):47–61
- Nazemosadat MJ, Ravan V, Kahya E, Ghaedamini H (2016) Projection of temperature and precipitation in Southern Iran using ECHAM5 simulations Iran. *J Sci Technol Trans Sci* 40:39–49
- Palizdan N, Falamarzi Y, Huang YF, Lee TS (2016) Precipitation trend analysis using discrete wave at the Langat River basin, Selangor, Malaysia. *Stoch Environ Res Risk Assess*. <https://doi.org/10.1007/s00477-016-1261-3>
- Palomino-Lemus R, Córdoba-Machado S, Gámiz-Fortis S, Castro-Díez Y, Esteban-Parra MJ (2015) Summer precipitation projections over northwestern South America from CMIP5 models. *Glob Planet Chang* 131:11–23
- Partal T, Kahya E (2006) Trend analysis in Turkish precipitation data. *Hydrol Process* 20:2011–2026
- Pettitt AN (1979) A non-parametric approach to the change point problem. *J Appl Stat* 28:126–135
- Rahimzadeh F, Asgari A, Fattahi E (2009) Variability of extreme temperature and precipitation in Iran during recent decades. *Int J Climatol* 29:329–343
- Ramos MC, Balasch JC, Martínez-Casasnovas JA (2012) Seasonal temperature and precipitation variability during the last 60 years in a Mediterranean climate area of Northeastern Spain: a multivariate analysis. *Theor Appl Climatol* 110:35–53
- Raziei T, Daryabari J, Bordi I, Pereira LS (2014) Spatial patterns and temporal trends of precipitation in Iran. *Theor Appl Climatol* 115(3):531–540
- Roshan GR, Grab SW (2012) Regional climate change scenarios and their impacts on water requirements for wheat production in Iran. *Int J Plant Prod* 6:239–266
- Roshan GR, Khoshakhlagh F, Azizi G (2012) Assessment of suitable general atmosphere circulation models for forecasting temperature and precipitation amounts in Iran under condition of global warming. *Geogr Dev* 27:5–7
- Scardilli AS, Llano MP, Vargas WM (2015) Temporal analysis of precipitation and rain spells in Argentinian centenary reference stations. *Theor Appl Climatol*. <https://doi.org/10.1007/s00704-015-1631-7>
- Schlunzen KH, Hoffmann P, Rosenhagen G, Rieckeb W (2010) Long-term changes and regional differences in temperature and precipitation in the metropolitan area of Hamburg. *Int J Climatol* 30:1121–1136
- Sen PK (1968) Estimates of the regression coefficient based on Kendall's tau. *J Am Stat Assoc* 63(324):1379–1389
- Sharmila S, Joseph S, Sahai AK, Abhilash S, Chattopadhyay R (2015) Future projection of Indian summer monsoon variability under climate change scenario: an assessment from CMIP5 climate models. *Glob Planet Chang* 124:62–78
- Sheikha V, Bahremanda A (2011) Trends in precipitation and stream flow in the semi-arid region of Atrak river basin, North Khorasan, Iran. *Desert* 16:49–60
- Shifteh Some'e B, Ezani A, Tabari H (2012) Spatiotemporal trends and change point of precipitation in Iran. *Atmos Res* 113:1–12
- Sneyers S (1990) On the statistical analysis of series of observations; technical note no. 143, WMO No. 725 415, secretariat of the World Meteorological Organization, Geneva, p 192
- Tabari H, Aghajanloo MB (2013) Temporal pattern of aridity index in Iran with considering precipitation and evapotranspiration trends. *Int J Climatol* 33(2):396–409
- Tabari H, Hosseinzadeh Talaei P (2011a) Spatiotemporal trends and change point of precipitation in Iran. *J Hydrol* 396:313–320
- Tabari H, Hosseinzadeh Talaei P (2011b) Recent trends of mean maximum and minimum air temperatures in the western half of Iran. *Meteorol Atmos Phys* 111:121–131
- Tabari H, Shifteh Some'e B, Rezaeian Zadeh M (2011) Testing for long-term trends in climatic variables in Iran. *Atmos Res* 100:132–140
- Tabari H, Abghari H, Hosseinzadeh Talaei P (2012a) Temporal trends and spatial characteristics of drought and rainfall in arid and semi-arid regions of Iran. *Hydrol Process* 26:3351–3361
- Tabari H, Hosseinzadeh Talaei P, Ezani A, Some'e BS (2012b) Changes and monotonic trends in autocorrelated temperature series over Iran. *Theor Appl Climatol* 109:95–108
- Tabari H, AghaKouchak A, Willems P (2014) A perturbation approach for assessing trends in precipitation extremes across Iran. *J Hydrol* 519:1420–1427
- Tabari H, Taye MT, Willems P (2016) Statistical assessment of precipitation trends in the upper Blue Nile river basin. *Stoch Environ Res Risk Assess*. <https://doi.org/10.1007/s00477-015-1046-0>
- Taylor KE, Stouffer RJ, Meehl GA (2009) A summary of the CMIP5 experiment design. *PCDMI Rep.*, pp 33. Available online at http://cmippcmdi.llnl.gov/cmip5/docs/Taylor_CMIP5_design.pdf
- Terink W, Willem W, Droogers P (2013) Climate change projections of precipitation and reference evapotranspiration for the Middle East and Northern Africa until 2050. *Int J Climatol* 33(1430):3055–3072. <https://doi.org/10.1002/joc.3650>
- von Storch H (1995) Misuses of statistical analysis in climate research. In: Storch HV, Navarra A (eds) *Analysis of climate variability: applications of statistical techniques*. Springer, Berlin, pp 11–26
- Wei K, Bao Q (2012) Projections of the East Asian winter monsoon under the IPCC AR5 scenarios using a coupled model: IAP-FGOALS. *Adv Atmos Sci* 29(6):1200–1213
- Xu K, Milliman JD, Xu H (2010) Temporal trend of precipitation and runoff in major Chinese rivers since 1951. *Glob Planet Chang* 73(3–4):219–223
- Yao J, Chen Y (2015) Trend analysis of temperature and precipitation in the Syr Darya basin in Central Asia. *Theor Appl Climatol* 120:521–531
- Yavuz H, Erdoğan S (2012) Spatial analysis of monthly and annual precipitation trends in Turkey. *Water Resour Manag* 26:609–621
- Zarenistanak M, Dhorde A, Kripalani RH (2014a) Temperature analysis over southwest Iran: trends and projections. *Theor Appl Climatol* 116:103–117
- Zarenistanak M, Dhorde AG, Kripalani RH (2014b) Trend analysis and change point detection of annual and seasonal precipitation and temperature series over southwest Iran. *J Earth Syst Sci* 123(2):281–295

Zarenistanak M, Dhorde AG, Kripalani RH, Dhorde AA (2015) Trends and projections of temperature, precipitation, and snow cover during snow cover-observed period over southwestern Iran. *Theor Appl Climatol* 122(3):421–440

Zhao L, Xu J, Powell AM, Jiang Z (2015) Uncertainties of the global-to-regional temperature and precipitation simulations in CMIP5 models for past and future 100 years. *Theor Appl Climatol* 122:259–270